



Monitoring Chip Formation in Machining through Strategical On-line Signal Processing of Acoustic Emission

R. Margot¹, A. M. G. Boeira¹, F. Kuster¹, H. Roelofs², U. Urlau², W. L. Weingaertner³

¹ *Institute of Machine Tools and Manufacturing, Department for Mechanical and Process Engineering,
Swiss Federal Institute of Technology, 8092 Zürich, SWITZERLAND*

² *von Moos Stahl AG, 6021 Emmenbrücke, SWITZERLAND*

³ *Laboratory of Precision Mechanics, Department of Mechanical Engineering, Federal University of Santa Catarina
88040-970 Florianópolis, BRASIL*

The 38th CIRP International Seminar on Manufacturing Systems May 16/18 - 2005

Monitoring Chip Formation in Machining through Strategical On-line Signal Processing of Acoustic Emission

R. Margot¹, A. M. G. Boeira¹, F. Kuster¹, H. Roelofs², U. Urlau², W. L. Weingaertner³

¹ Institute of Machine Tools and Manufacturing, Department for Mechanical and Process Engineering, Swiss Federal Institute of Technology, Zurich, Switzerland

² von Moos Stahl, Emmenbrücke, Switzerland

³ Laboratory of Precision Mechanics, Department of Mechanical Engineering, Federal University of Santa Catarina, Florianópolis, Brasil

Abstract

Although acoustic emission (AE) sensors are acquiring high frequency accelerations the signal acquisition and interpretation is challenging. Without any on-line signal processing strategy the amount of data will expand fast when recording the MHz bandwidth rough signal. For applications under industrial conditions a practical strategy relies on the root mean square (RMS) method which is reducing the amount of data. Vibrations due to the tool device, work-piece and machine are disturbing the measurement of the cutting process that cannot be separated after the RMS processing. For a reliable process monitoring the signal has to be as clear as possible, and so the signal needs to be conditioned on-line before the RMS is taken.

Keywords:

Acoustic Emission, Monitoring, Chip Formation, Friction

1 INTRODUCTION

A piezo-electrical sensor is measuring a mechanical stress in form of a pressure, an acceleration or an acoustic emission (AE). The displacement of charges (Figure 1) in the piezo element is evaluated through a charge amplifier.

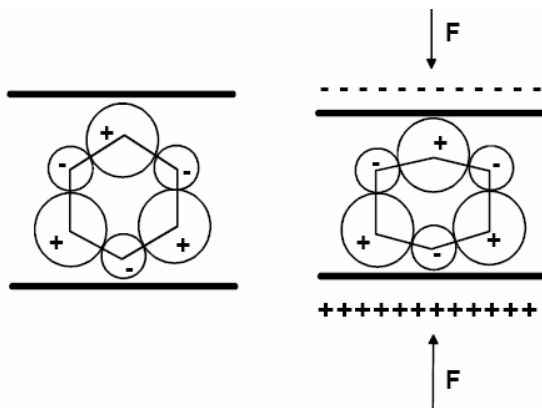


Figure 1: Displacement of charges for a quartz crystal.

Mechanically the charges are not measuring an acceleration directly but a force, which is interpreted as an acceleration using the 2nd law of Newton: $F = ma$.

Recording the charges in a machining environment, many sources of disturbances [1] (Figure 2) occur preventing a simple interpretation of AE signals. It is the researchers challenge to find an adequate strategy in measuring, treating and interpreting the AE information. In the past such strategies have been obtained by focussing on the dominant AE peaks [2] representing chip breaks in the machining process. In addition the present work takes also small signals due to frictional interaction into consideration. Applying a simple geometrical model, information about the tool-chip friction can then be gained immediately during machining.

The transmission of information in presence of noise is still possible if the system corrects the errors [3].

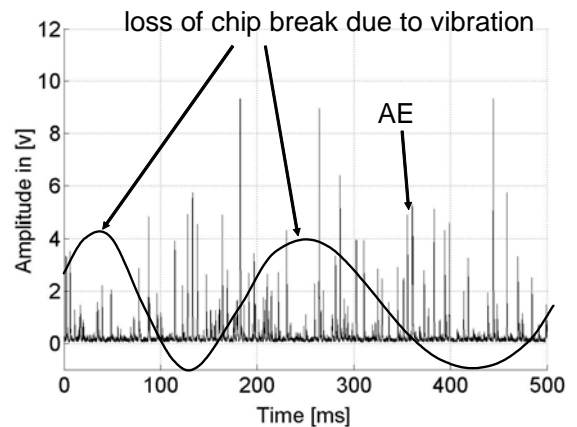


Figure 2: Loss of information without strategy.

1.1 Chip formation

The chip is formed by a tool-workpiece interaction (Figure 3). As the edge of the tool penetrates into the workpiece, the material ahead of the tool is sheared. The sheared material or chip partially deforms and moves along the rake face of the tool. The high strain rates modify the chip cross-section. The cutting analyses at the tool-workpiece-chip interfaces show the existence of 4 zones [4].

1. The primary shearing zone.
2. The secondary shearing zone.
3. The principal and secondary clearance zone.
4. The dead zone.

Filtering out low frequent signals (due to vibrations of machine components) the following sources of AE signals are expected:

- Chip breaks.
- Internal friction (zone 1).
- Chip-tool interaction (dominant zone 2).
- Workpiece-tool interaction (zone 3).

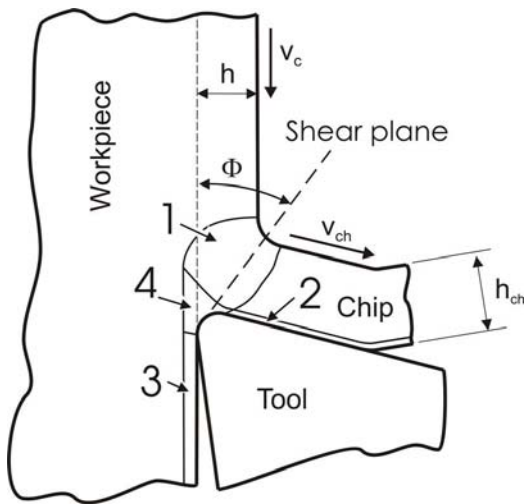


Figure 3: Chip formation zone. A main source for AE is the secondary shearing zone [5].

Where:

h = Undeformed chip thickness.

h_{ch} = Chip thickness.

v_c = Cutting speed.

v_{ch} = Chip speed.

Φ = Shear angle.

All these events cause AE signals in the same frequency range but the corresponding AE amplitudes differ clearly. Chip breaks lead to huge AE amplitudes which allow to subtract this part from the AE signal. The internal friction and the work piece-tool interaction are supposed to be negligible in comparison to the chip-tool interaction. Under these assumptions a straight forward strategy can be chosen to extract information about the chip tool friction.

2 STRATEGY

Strategies described by Kluff [6] and Lang [7] rely on teaching methods. The new strategy reduces stochastic disturbances mentioned by Chen [1] and set a dynamic detection level. An appropriated signal processing chain is used in order to filter the signal electronically as well as mechanically. After a band pass filter between 500 kHz and 1000 kHz the RMS of AE signal is built [8]. Then chip breaks can be detected from the remaining signal. A nominal chip length is computed by multiplying the time between two chip breaks by the cutting speed. The strategy (Figure 4) consists in acquiring process information in a machine environment to make the process reliable [9],[10]. There are two sides for the AE measurement: the tool side and the workpiece side. As AE information is located in very high frequencies (MHz domain [11]), it is not suited to traverse a ball bearing. Almost only the natural frequency of the ball bearing will be transmitted by AE.

Therefore a non rotative device will be chosen for the AE sensor. For example in turning the AE sensor will be mounted on tool side and for drilling on the workpiece side but before any ball bearing.

At this stage the optimal sensor position is found. Nevertheless the clamping devices, tool and workpiece are to be considered too [5], when the process generates high vibration level [12] which is the case for worn tool, for roughing operations and for drill operations. To avoid

saturation for AE measurement under strong vibrations, high pass filters are used.

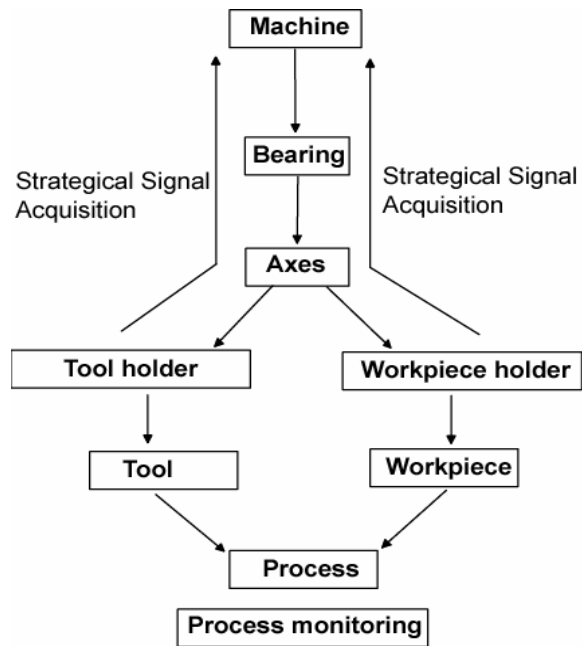


Figure 4: Strategy.

2.1 Mechanical filter

The situation for AE in such environment is like trying to write a letter by hand in a tractor. If the tractor is working in a field big waves will destroy the hand writing with disturbance in the text, which will appear stochastically. If the tractor is moving on a good road the text will be clearer like in the finishing operation. But if you are in a cruise boat you can write very clearly even if there is a storm outside. The mass of the water will damp the vibrations of the waves on the see. As the electronic filters are processing the signal after sensing AE, mechanical filter (Figure 5) is used to damp strong vibrations mentioned above in order to prevent saturations of the AE sensor (loss of chip break information [13]). The mechanical filter is realized by an oil pot.

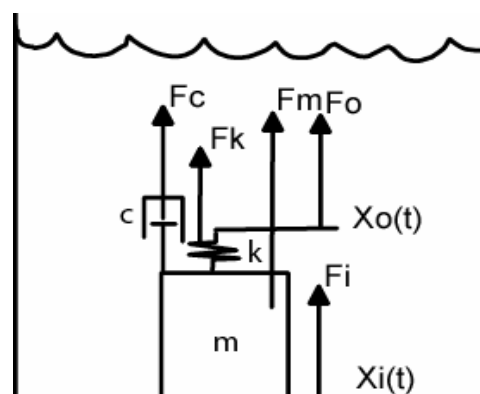


Figure 5: Mechanical high pass filter.

Where:

c = Damping of oil.

k = Stiffness of oil.

m = Mass of oil.

$$H(s) = \frac{\frac{m}{k}s^2}{1 + \frac{c}{k}s + \frac{m}{k}s^2} = \frac{X_o}{X_i} \quad (1)$$

For the comparison and for the computation, the equivalent electronic filter (Figure 6) will be used as a model.

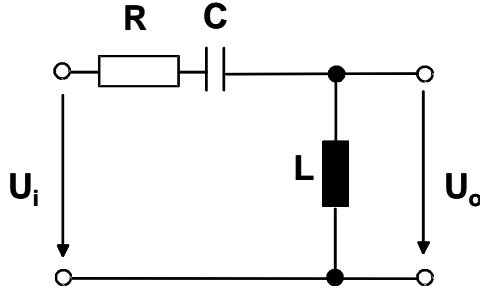


Figure 6: Corresponding electronic filter.

$$H(s) = \frac{s^2 LC}{1 + sRC + s^2 LC} = \frac{U_o}{U_i} \quad (2)$$

The transfer function of electronic devices has been studied more than mechanical ones. They help to understand how an oil pot is functioning (Figure 7).

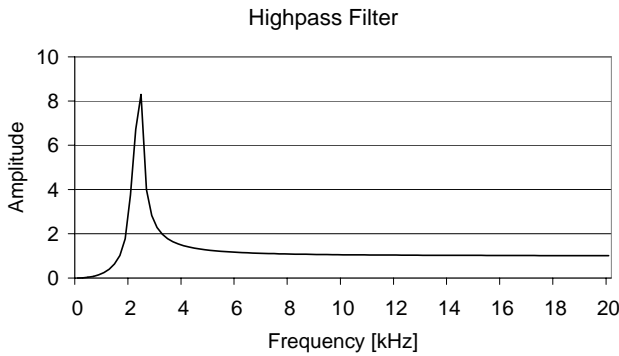


Figure 7: Frequency response of the oil pot.

2.2 Electronic filter

On one hand Chen [1] mentions disturbances of AE in his conclusion: "Signals are accompanied with a lot of additional confusing data. In order to provide an accurate interpretation or feature extraction of the information produced an advanced signal processing and analysis is needed". On the other hand Shannon [3] calls these confusing data "equivocation" or uncertainty of a signal Y received when a signal X is sent $H(X|Y)$. The electronic filter is selecting the band-width range from 0.5 to 1 MHz (0.1 to 1 MHz in drilling) of the AE signal and implements an on-line error correcting code on the signal amplitude. In this range the frequencies of the machine components disappear and the signal for the process monitoring is not mixed with other unwanted signals. After the filtering, further signal processing, which is usually irreversible like the RMS value, will not mix those additional disturbances

and thus the AE signal will not be confused. The first step after the band pass filter is provided by the taking the RMS value [8], the second by the low pass filter 3 kHz. These operations are needed for the on-line processing of AE. Otherwise the costs rise by dealing with high frequency data acquisition and unnecessary data handling.

2.3 Data reduction

Suppose a finishing cut of feed rate $f=0.05$ mm/rev with a cutting speed of $v_c=200$ m/min, a length of cut $l=30$ mm and a diameter of $d=26$ mm. We have process time of 15 s.

$$t = \frac{l}{\frac{v_c}{\pi d} f} = 15 \text{ s} \quad (3)$$

Without signal conditioning the amount of data of the original AE-signal of a process time of 15 s will be very large.

$$15 \times 2 \text{ MHz} \times 4 \text{ Bytes} = 120 \text{ Mbytes} \quad (4)$$

This big amount of data is due to the high frequency range of AE and because of the Nyquist [14]-Shannon [15] sampling theorem, where the sampling rate is twice of the signal frequency content. Indeed, if only the chip breaks with AE friction are recorded, the on-line signal processing will reduce this amount. For this purpose, the chip break is transformed in a peak by taking the RMS (Figure 8).

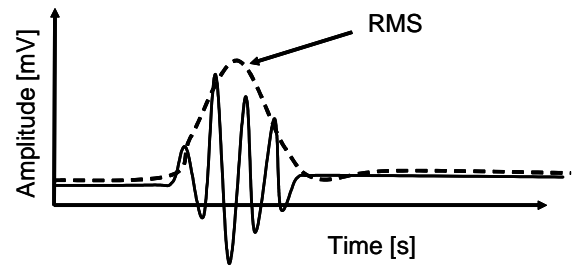


Figure 8: AE-Peak by taking the RMS.

The RMS procedure (Figure 9) is free of confusion if the lower frequencies are removed before.

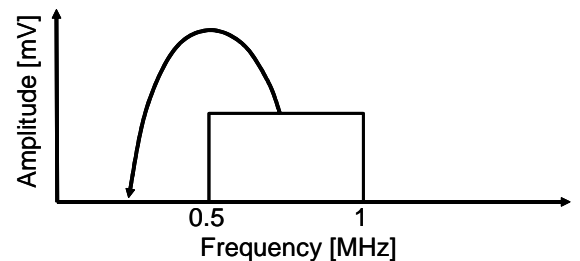


Figure 9: Frequency application of the RMS.

2.4 Realisation

The AE-Sensor is bathed with oil in a steel pot (Figure 10) and mounted on the tool holder approximately 100 mm far from the tool insert.



Figure 10: Kistler AE sensor 8152B in an oil pot as high pass filter.

2.5 Signal chain

The signal content of AE is characterized mainly by chip breaks, spindle noise, structural vibration and friction (Figure 11).

After filtering the AE-Signal with mechanical high pass and electrical band pass (BP) filter between 0.5 and 1 MHz, the RMS is built (Figure 12).

$$RMS(BP(AE(t))) = RMS(BP(B(t) + R(t) + N(t) + S(t))) \quad (5)$$

$$RMS(BP(AE(t))) = RMS(BP(B(t) + R(t))) \quad (6)$$

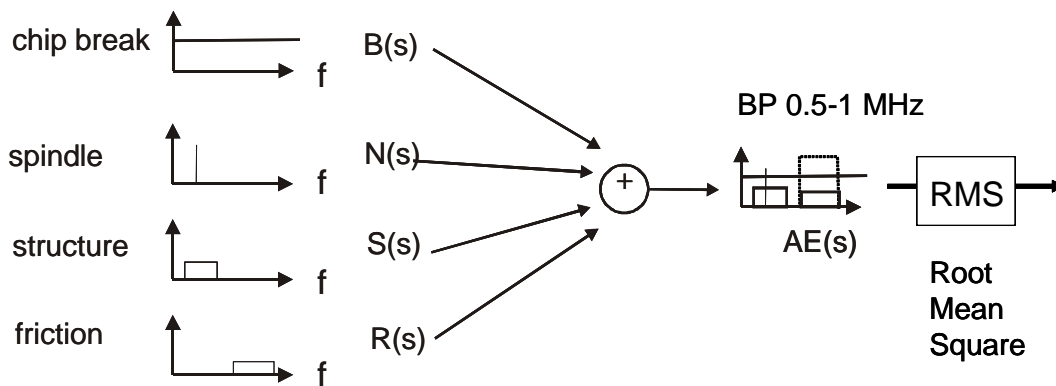


Figure 11: AE signal content.

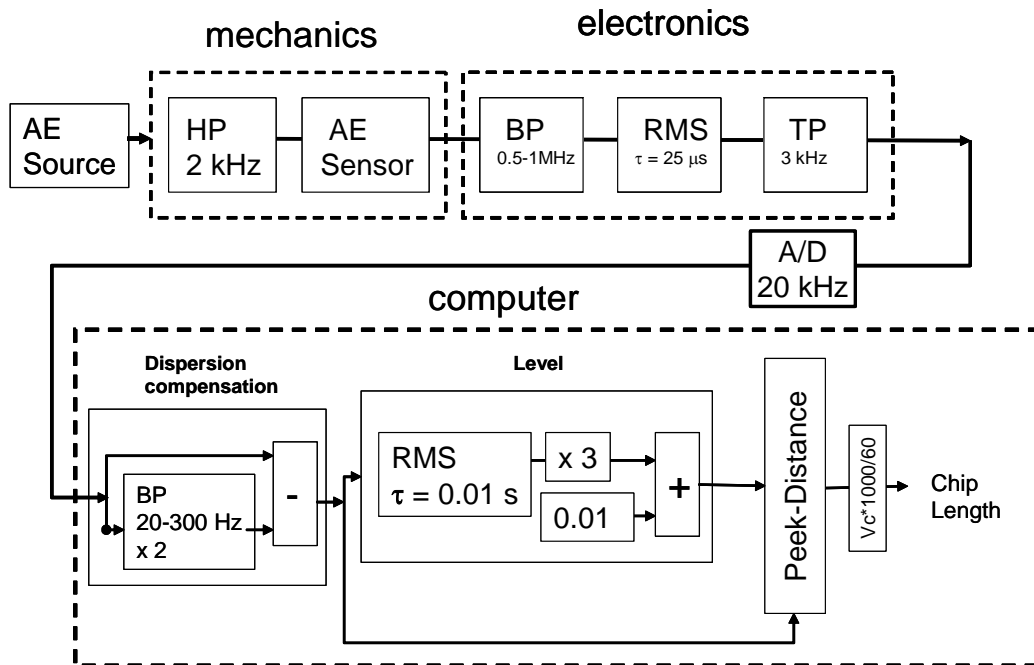


Figure 12: Signal chain for turning.

The AE-Signal is now ready to be processed further and analysed. There are no holes in the Signal, because the AE-sensor is no more saturated. By using a low pass-filter and multiplying this signal with a factor of 3 for turning (Algorithm in [2]), and 30 for drilling, the chip breaks are detected reliably (Figure 13).

3 MODEL OF FRICTION

The interface considered is between the chip and the tool rake face [5].

The roughness between the tool surface and the chip can be characterized by a depth of value R_f .

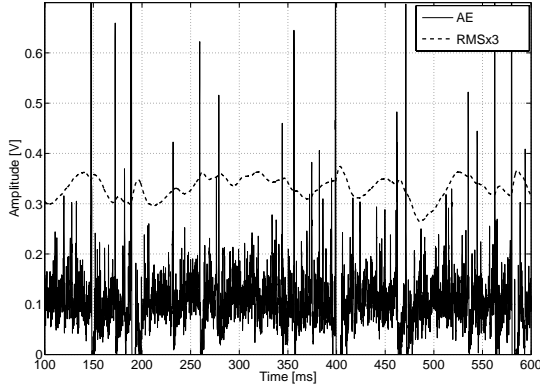


Figure 13: Automatic recognition of chip breaks.

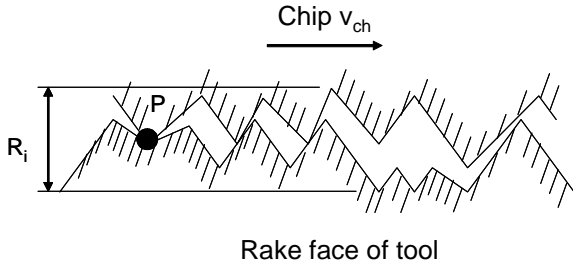


Figure 14: Interface between chip and tool rake face.

At the contact point P an AE acceleration will be generated:

$$F = m_{AE} a = k_p \frac{R_i}{2} \quad (7)$$

With the assumption that R_i has a normal distribution.

At the total surface contact, n points contribute to the AE-Signal. If AE is proportional to the acceleration a .

$$a = \frac{k_s}{m_{AE}} \cdot \frac{R_i}{2} \quad (8)$$

Where:

$$k_s = nk_p = \text{Stiffness of the surface} \quad (9)$$

Equation 8 shows that AE is distributed proportional to the surface stiffness k_s of the chip (the die surface stiffness of the tool stiffer) and to the roughness $\frac{R_i}{2}$ between the roughness of the chip R_s , the coated tool tip depending of wear.

As k_s is proportional to the hardness e.g. to the hardness Vickers HV.

$$RMS_{AE} \propto HV_{WP} \cdot R_s \cdot \text{Coating} \cdot \text{Wear} \quad (10)$$

For convenience this RMS_{AE} will be represented by AER meaning the AE noise friction.

The friction model takes in account the friction mechanisms [13]:

- I Elastic entrance of the material (HV_{WP}, R_s)
- II Plastic entrance of the material (HV_{WP}, R_s)
- III Micro cut of the material (coating)
- IV Micro breaking in the stick layers (wear)
- V Fatigue and breakage of the base material (chip break).

The AE coming from zone Z_1 , Z_3 and Z_4 is of smaller amplitude as that of Z_2 and are as following negligible.

$$RMS(Z_2 + Z_3) = \sqrt{E(Z_2^2) + E(Z_3^2) + E(2Z_2Z_3)} \quad (11)$$

Where:

E = Expected value.

Z_2 and Z_3 are statistically independent as they come from two different source of AE, $E(2Z_2Z_3) = 0$.

$$RMS(Z_2 + Z_3) = \sqrt{RMS(Z_2)^2 + RMS(Z_3)^2} \quad (12)$$

When $Z_3 \ll Z_2$, the hypotenuse equals the big edge.

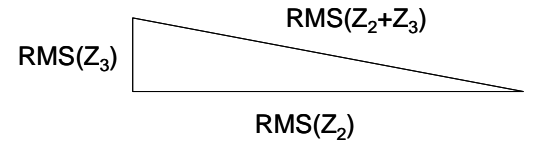


Figure 15: RMS of 2 sources of AE.

Therefore the AE sensor acquires on the tool side almost only the friction between the chip and the tool (zone Z_2). This part corresponds to the roughness of the chip R_s .

$$h_s = \frac{s}{\sin(\Phi)} \quad (13)$$

$$l_s = \frac{h}{\sin(\Phi)} \quad (14)$$

$$AER \propto al + bh_s = a \frac{h}{\sin(\Phi)} + b \frac{s}{\sin(\Phi)} \quad (15)$$

$$AER \propto \frac{ah + bs}{\sin(\Phi)} = \frac{c}{\sin(\Phi)} \quad (16)$$

Where a , b and c are weighting constants of the vibration parts.

$$R_s = \frac{c}{\sin(\Phi)} \quad (17)$$

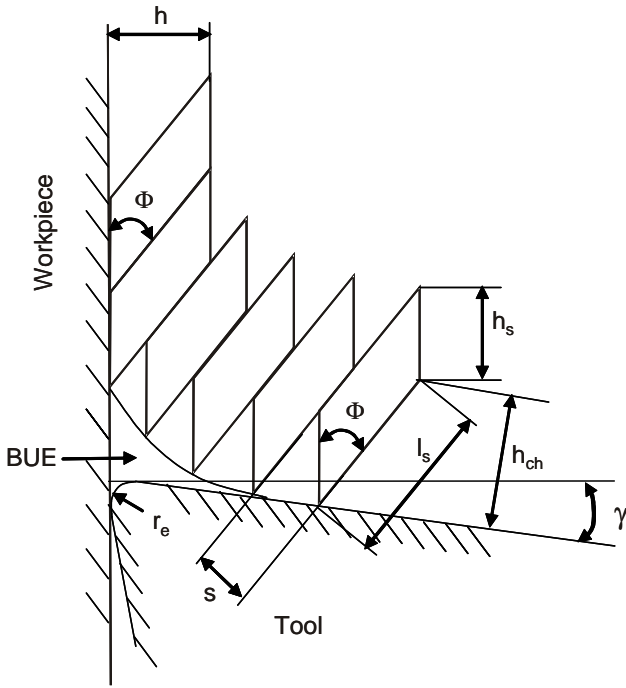


Figure 16: Chip formation [4],16,17].

The geometrical description of the surface combined with the elastic-plastic behaviour of the chip described by its hardness, gives the AER relation. Applying equations 10 and 17, the RMS-value of the AE signal becomes a function of the hardness of the material, the coating of the tool, the wear and the shear angle (considering fixed cutting conditions like cutting speed, depth of cut and tool geometry).

$$AER_{fric} \propto HV_{wp} \frac{c}{\sin(\Phi)} \cdot \text{coating} \cdot \text{wear} \quad (18)$$

The AE noise can be directly correlated with the friction coefficient, which is depending on the coating and wear.

$$AER_{fric} = k \cdot HV_{WP} \cdot \frac{1}{\sin(\Phi)} \mu \quad (19)$$

In the frequency range of 0.5-1MHz the features of the AE friction as well as the chip breaks are in the signal. The AE breaks may be filtered low-pass, but they will add a DC part by the short chip in the AE friction. They are taken away by subtraction all peak higher than the dynamic level 3x RMS.

4 RESULTS

The presented new method has been applied in turning tests as well in drilling studies. Investigations at 200 m/min single point turning were performed to measure the friction coefficient on-line. The friction coefficients from this analysis were compared with friction coefficients from force evaluations.

4.1 AE noise and friction

The filtered chip-tool AE noise signal has been recorded for 3 different types of steel and 3 tool tips with different coatings at fixed turning conditions ($v_c=200$ m/min, $a_p = 2$ mm, $f = 0.2$ mm/rev, dry machining) and tool geometry (CNMG 120408). Although the tool coating consists of a

multilayer only the outer layer ("uncoated", "TiN" or "Al₂O₃") is decisive for friction and hereafter referenced. The compositions of the low carbon free cutting steels are given in Table 1.

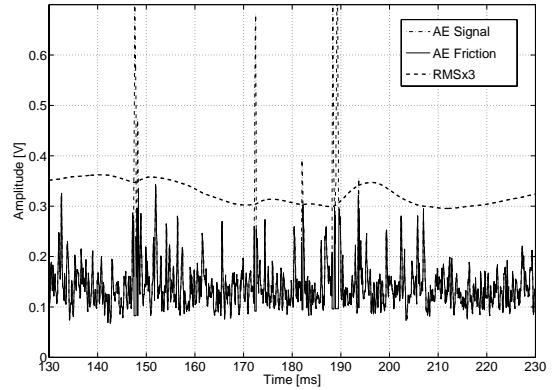


Figure 17: After removing chip breaks, the Signal is interpolated and the RMS of the remaining Signal gives the acoustic friction.

	C	S	Mn	Si	P	Bi	Sn
Steel 1	0.09	0.38	1.47	0.16	0.011	-	-
Steel 2	0.09	0.31	1.03	0.003	0.062	0.078	-
Steel 3	0.09	0.30	1.13	0.006	0.058	-	0.054

Table 1: Composition of tested steels [%].

Every steel has been characterized by micro hardness measurements which allow indentations in the area of interest in the turning test.

The shear angle Φ has been calculated from the chip thickness (averaged out of five manually measured values with Equation 20).

$$\frac{\cos(\Phi - \gamma)}{\sin(\Phi)} = \lambda_h = \frac{h_{ch}}{h} \quad (20)$$

The friction coefficient μ has been determined by force measurement [16].

Steel	Tool tip	HV	Φ [°]	μ
1	Al ₂ O ₃	187	25°	0.37
	none	187	23°	0.46
	TiN	187	25°	0.39
2	Al ₂ O ₃	190	25°	0.39
	none	190	24°	0.50
	TiN	190	25°	0.41
3	Al ₂ O ₃	183	26°	0.39
	none	183	25°	0.50
	TiN	183	27°	0.43

Table 2: Input data for the model calculation.

In Figure 22 the measured RMS value of the AER signal is compared with the AER_{fric} as calculated by Equation 19. The trend between AER_{fric} and $AER_{measured}$ is quite promising. The AER signal clearly shows the influence of tool coating. In both evaluation methods the friction is lowest for the Al_2O_3 coated tool followed by the TiN coated and the uncoated tool. The uncoated tools give a higher AER signal than the coated ones and the scattering of data is more severe. The reason for this data scattering is still under investigation. Using uncoated tools higher friction frequencies moving out of the recorded frequency band might occur. This is supposed to be a potential “source of error”.

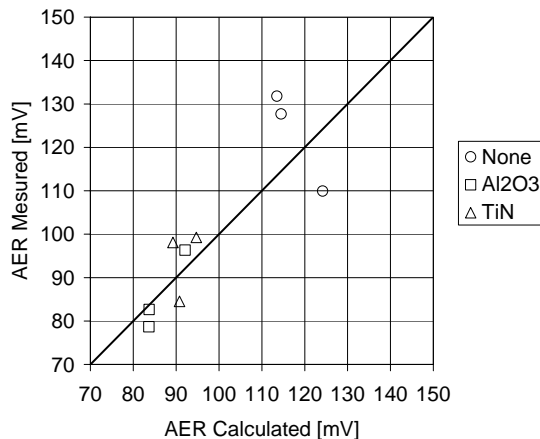


Figure 18: AER measured compared with the AER_{fric} model calibrated over all points with $k=0.53$.

4.2 Built-up edge (BUE) formation during turning

Not only the “noise contribution” to the AE signal can be used for on-line process control but also the AE peaks due to chip breaking [2]. For example irregularities in the chip forming process due to BUE are reflected in chip length changes.

BUE formation takes place at low cutting speeds (see Figure 23). For the investigated low carbon free cutting steels this happens typically in a speed range of 20 – 50 m/min (depending on particular turning conditions). Under such conditions the turning operation is characterized by the presence of tiny powder like chips coming from the decay of BUE. This phenomena can be detected by a Chip Control System [2] allowing an on-line observation. Figure 20 shows a data collection of an on-line chip length measurement. On the y-axis the number of registered chips in a fixed time interval (x-axis) is given. As additional information the chip lengths are indicated by colours. Bright colours mark small chips. The circle surrounds the area of BUE formation where an increased number of small chips is found.

Figure 21 gives the optical verification of the measured result. Between the regular chips from the chip forming and breaking process powder like chips from the breakup of BUE can clearly be seen.

4.3 Built-up edge formation during drilling

In drilling the cutting speed varies along the cutting edge. There is no fixed cutting speed over the cutting edge resulting in a chip formation behaviour that differs completely from the turning process. Under BUE conditions an increase in chip length is found. Although this behaviour couldn't be really observed on-line the Chip Control System gives again a good visualisation.

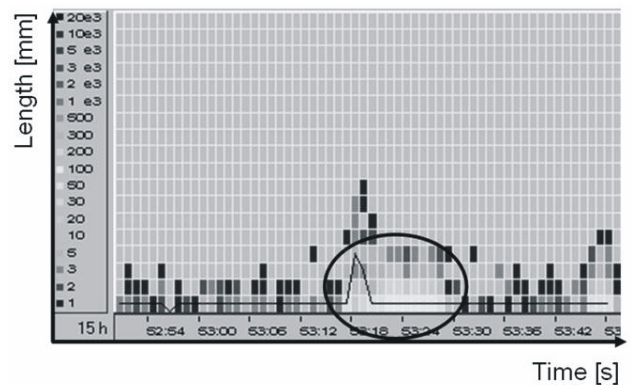


Figure 19: Built-up edge monitoring with the chip length system, without lubrication, coating Al_2O_3 , $v_c=20$ m/min, $a_p=2$ mm, $f=0.1$ mm/rev in steel 1.

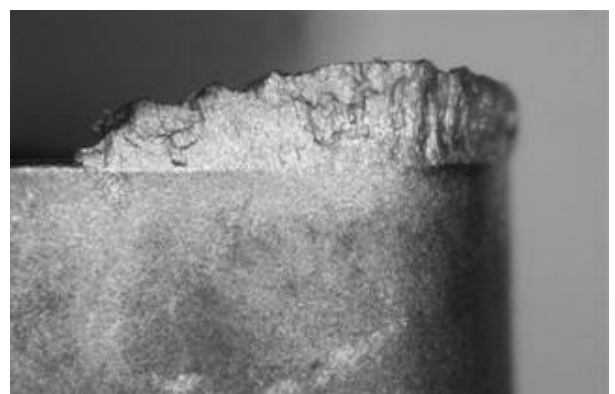


Figure 20: Built-up edge on a Al_2O_3 coated insert.

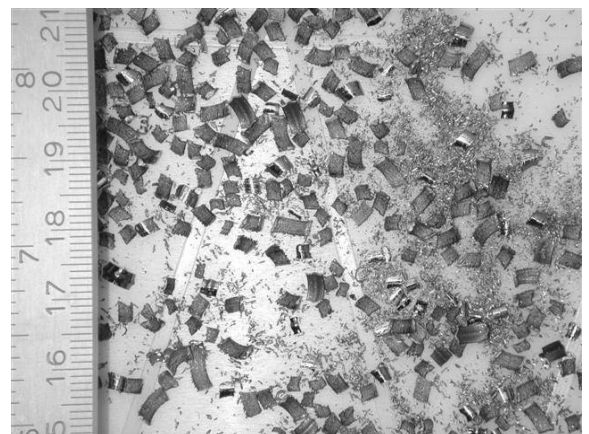


Figure 21: Powder chip when forming BUE.

5 CONCLUSION

The strategy presented has been effective for monitoring and analysing chip building in a noisy environment. From the AE signal the contributions due to chip breaking could be separated and interpreted successfully. The subtracted AE noise level contains further useful information about friction. Applying a simple model a first attempt was started to extract the chip tool friction coefficient. For further improvement more data are necessary. Future work will therefore include the acquisition of more data in machining and thus characterising steels, lubricant and tools for industrial database.

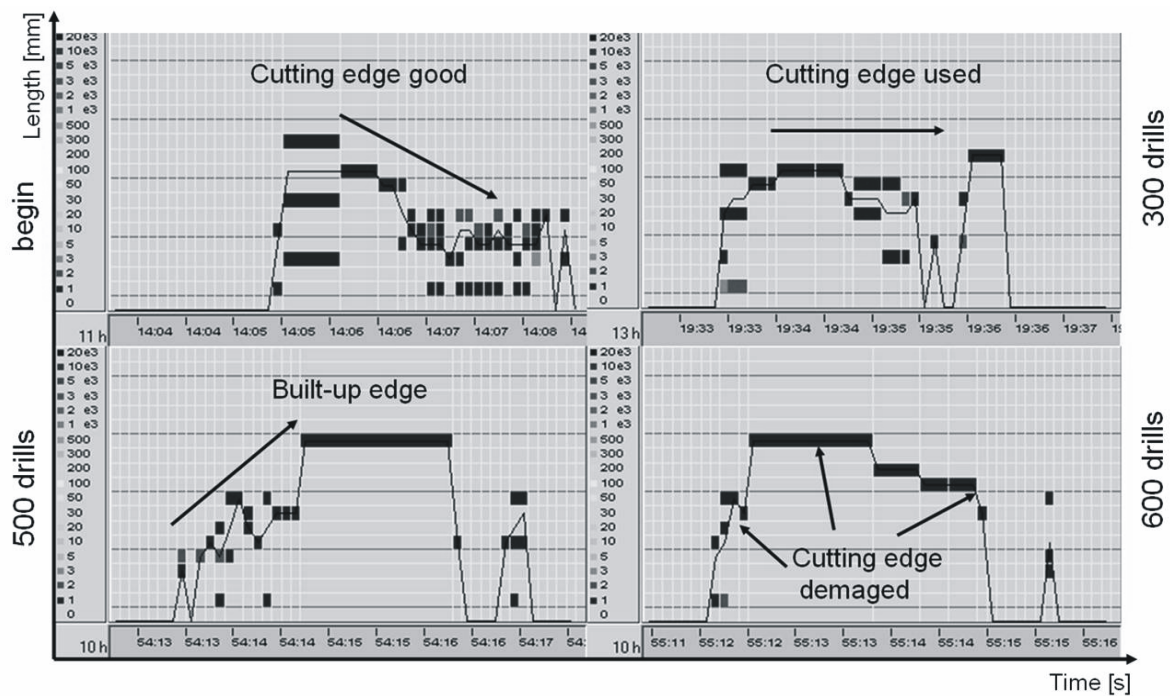


Figure 22: BUE monitored by Chiplength monitoring System for drilling, HSCO 6.000 mm, uncoated, $v_c = 30$ m/min, $f = 250$ mm/min, in St37, lubricated.

6 ACKNOWLEDGMENT

This research was supported by von Moos Stahl AG, Blaser Swissslube AG, Kistler Instrumente AG, Iscar Hartmetall AG, Gühring oHG, and the commission for technology and innovation (CTI). The authors would like to thank them for their cooperation.

7 REFERENCES

- [1] Chen, X. Z. H., Wildermuth, D., 2001, In-Process Tool Monitoring through Acoustic Emission Sensing Automated Material Processing Group, Automation Technology Division.
- [2] Kuster, F., Margot, R., 2002, Online-Spanlängenerkennung beim Drehen, Schweizer Maschinenmarkt Nr. 45, pp. 93-95.
- [3] Shannon, C. E., 1948, A Mathematical Theory of Communication, The Bell System Technical Journal, Vol. 27, pp. 379-423, 623-656, July, October
- [4] Jawahir, I.S., van Luttervelt, C.A., 1993, Recent Developments in Chip Control Research and Applications, CIRP, 42/2:659-693.
- [5] British Steel, 1999, Development of a new machinability test methodology/machining model for improved free cutting steels, ECSC research contract 7210.MA/821, EUR 18617.
- [6] Kluft, W., 2001, Die richtige Strategie für die Werkzeugüberwachung, Aachen, WB 3
- [7] Lange, D., 2002, Hohe Produktivität durch Prozessüberwachung, Artis, www.artis.de
- [8] Scheer, C., 2000, Überwachung des Zerspanprozesses mit geometrisch bestimmter Schneide durch Schallemissionsmessung, Diss. Nr. 13462 ETH Zürich
- [9] Margot, R., et al; 1998, Using Machine Control Information for Reliable Process Monitoring, CIRP International seminar on Intelligent Computation in Manufacturing Engineering, Capri, Italy, 1-3 July, pp. 523-529
- [10] Weinert, K., Löbke, H., Webber, O., 2000, Spanüberwachung sichert Prozess Technica 24, pp. 16-21
- [11] Hundt, W., 1996, Ein Beitrag zur Beobachtung von Schleifprozessen mittels Schallemission, Diss. Nr. 11864 ETH Zürich
- [12] Chiou, R. Y., Liang, S. Y., 2000, Analysis of acoustic emission in chatter vibration with tool wear effect in turning, International Journal of Machine Tools & Manufacture, 40 pp. 927-941
- [13] Maus, D., 2003, Identifikation und Modellierung nichtlinear-dynamischer Effekte in spanenden Prozessen, Kaiserslautern Dissertation Band 48
- [14] Nyquist, H., 1928, Certain Topics in Telegraph Transmission Theory, Transaction of the A.I.E.E., pp. 617-644
- [15] Shannon, C. E., 1949, Communication in the Presence of Noise, Proceedings of the IRE, Vol. 37, no. 1, pp. 10-21
- [16] Stemmer C. E. Ferramentas de corte I, 4. ed. Florianópolis: Ed. Da UFSC, 1995
- [17] Dautzenberg, J. H., Veenstra P. C., van der Wolf, A. C. H., 1981, The Minimum Energy Principle for the Cutting Process in Theory and Experiment, CIRP Vol. 30/1